18th European Symposium on Computer Aided Process Engineering – ESCAPE 18
Bertrand Braunschweig and Xavier Joulia (Editors)

Morphological Population Balance for Modelling Shape Evolution of Crystals Grown From Solution

Cai Y Ma, Xue Z Wang* and Kevin J Roberts
Institute of Particle Science and Engineering, University of Leeds, Leeds LS2 9JT, UK

Abstract

Crystals are particles structured with multiple faces that often have different surface chemistry and hence varied growth rates during crystallisation. It is possible to manipulate the growth of individual facets e.g. via the introduction of tailor-made additives which via changes in the molecular recognition for the different crystal habit faces effect a reduction in the growth rate of a specific face, providing a means for control of the shape as well the size of the final crystalline product. However the prediction of crystal shape has previously been restricted to single crystals. On the other hand, population balance (PB) modelling of crystallisation has traditionally been mono-dimensional, i.e. based on the assumption that the crystals in a reactor all have a spherical shape. Recently a few researchers have reported two-dimensional (e.g. length and width) PB modelling for rod-like crystals. This paper presents a morphological (or polyhedral) population balance model for modelling the dynamic size evolution in all face directions. The morphological PB approach uses the crystal shape information for a single crystal obtained from morphology prediction or experiment as the initial face locations as well as face growth rates to predict the shape evolution of the crystal population. For every time instant during crystallisation, the shape prediction uses its shape at the last time moment and the growth rate of each face. The methodology is introduced by reference to potash alum ($KAl(SO_4)_2 \cdot 12H_2O$) for which literature data is available for comparison and validation.

Keywords: Morphological Population Balance, Morphology, Crystal Growth, Shape, Potash alum ($KAl(SO_4)_2 \cdot 12H_2O$), Shape Control

1. Introduction

Population balance (PB) modelling of the evolution of crystal size distribution with time in a reactor has mainly been restricted to using a mono-size definition, e.g. the volume equivalent diameters of spheres. This simplified treatment could lead to large errors in modelling crystallisation processes of crystals having needle-like or plate-like shape. In order to incorporate crystal shape information into PB modelling, a few researchers studied multidimensional PB but the published work has been restricted to two dimensions, e.g. length and width of rod like crystals(Ma, et al., 2002,Puel, et al., 2003a,Puel, et al., 2003b,Zhang and Lu, 2004,Briesen, 2006,Ma, et al., 2007,Wang, et al., 2007). In this study, a morphological (or polyhedral) PB model is presented which is able to incorporate more complicated crystal structures/shapes than rod-like crystals into PB modelling, therefore can simulate the size-related dimensional evolution of crystals for each face.

2. The Methodology

The mathematical formulation for multi-dimensional population balance has been discussed in literature, e.g. by Campos and Lage(Campos and Lage, 2003). Although in

literature, the so-called multi-dimension is often interpreted as mutliple-variables, i.e. a single size dimension as volume equivalent diameter plus other variables such as particle location, porosity and fraction ratio, the same mathematical formulation can be extended to include multiple size dimensions.

The mathematical formulation for multi-dimensional PB modelling, no matter employing a single size dimension plus other variables, or multiple size dimensions, can be given by Eq. (1):

$$\frac{\partial \psi(\vec{x},\vec{y},t)}{\partial t}+\nabla\cdot[\psi(\vec{x},\vec{y},t)\vec{v}]+\sum_{i=1}^{N}\frac{\partial}{\partial x_i}[\psi(\vec{x},\vec{y},t)G_i(\vec{x},\vec{y},t)] = B(\vec{x},\vec{y},t)-D(\vec{x},\vec{y},t)+R(\vec{x},\vec{y},t) \quad (1)$$

where N is the number of internal variables for a crystal, $\vec{x}$ is the internal variable vector with N components, which can be parameters related to crystal size, shape, and physical properties, $\vec{y}$ is the external variable vector with the corresponding components of spatial coordinates (y_1, y_2, y_3), ψ is the number population density function of crystals in the internal variable range (x_i, x_i+dx_i, i=1,N) and in the differential volume of $dy_1dy_2dy_3$, ∇ is the gradient operator for the $\vec{y}$ coordinates. The first term on the left hand side of Eq. (1) is the accumulation term of population, ψ. The second term donates the convection of population, ψ, in the $\vec{y}$ space with $\vec{v}$ being the velocity vector. The third term is the convection of population, ψ, due to growth of particle in the $\vec{x}$ space with G_i being the growth rate. On the right hand side of Eq. (1), the first and second terms represent the birth and death terms of population, ψ, due to all the processes during crystallisation such as aggregation, breakage, attrition etc. (excluding nucleation), and the third term is the nucleation term.

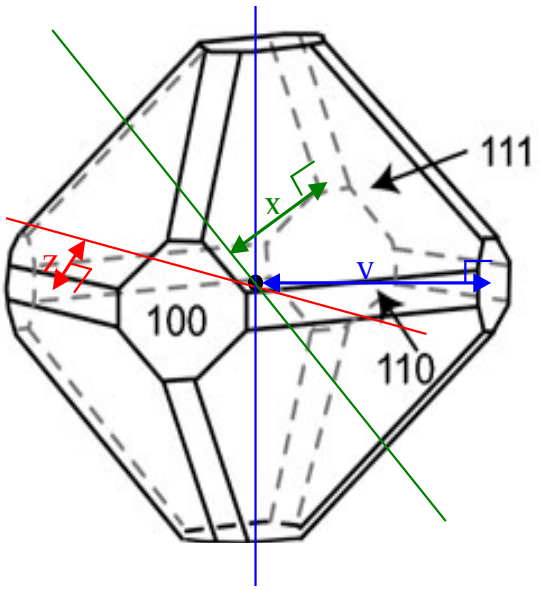

Fig. 1 The morphology of potash alum crystal and the three size characteristic parameters (x, y, z) used in a polyhedral PB model

In a well-mixed batch crystalliser, the influence of crystal positions in the crystalliser on population distributions can be removed. In addition, it is also assumed that agglomeration and breakage are negligible. Under these assumptions, a simplified version of Eq. (1) can be written as

$$\frac{1}{V_T(t)}\frac{\partial[\psi(\vec{x},t)V_T(t)}{\partial t}+\sum_{i=1}^{N}\frac{\partial}{\partial x_i}[\psi(\vec{x},t)G_i(\vec{x},t)] = R(\vec{x},t) \quad (2)$$

Noting that, from now on, the $\vec{x}$ in Eq. (2) is an N-dimensional vector which will only represent the size-related parameters of a crystal in order to distinguish the multi-dimensional PB model presented here from the other PB models which usually include only one size-related variable.

3. Morphological PB Modelling for Potash Alum

Taking into account a potash alum crystal having total 26 main habit faces (M = 26), a geometric centre can be found (Fig. 1). The normal distance from a crystal face to the geometric centre will form one dimension for a morphological PB model. In theory, a morphological PB model with 26 dimensions is needed, however, since some faces, such as the 8 {111} faces (M_1 = 8), are symmetry-related and supposed to the have same surrounding growth environment, hence same growth rates, these faces can be modelled as one dimension (x) in the PB model. Similarly, the 6 {100} faces (M_2 = 6) and 12 {110} faces (M_3 = 12) will form the second dimension, y, and third dimension, z, respectively. Therefore, the total number of independent faces identified is 3 (N=3), and a three-dimensional morphological PB model, corresponding to three parameters, x, y, z, shown in Fig. 1, can be fomulated. Noting that it is not necessary for the x, y, z parameters to be perpendicular to each other as they are only normal distances from three faces to the crystal centre. In this study, for simplicity, the effect of both primary and secondary nucleation of potash alum on population distributions was not considered. Under these assumptions equation of Eq. (2) can be written as,

$$\frac{1}{V_T(t)}\frac{\partial}{\partial t}\left[\psi(x,y,z,t)V_T(t)\right]+\frac{\partial}{\partial x}\left[G_1(x,t)\psi(x,y,z,t)\right]+\frac{\partial}{\partial y}\left[G_2(y,t)\psi(x,y,z,t)\right] + \frac{\partial}{\partial z}\left[G_3(z,t)\psi(x,y,z,t)\right]=0 \quad (3)$$

The first term is the accumulation term of population. The second, third and fourth terms are the population changes for the three main habit faces, respectively.

Crystal growth for potash alum has been studied in literature by a number of researchers (Read and Shockley, 1950,Vanderheijden and Vandereerden, 1992,Ristic, et al., 1996,Ristic, et al., 1997,Lacmann, et al., 1999,Klapper, et al., 2002)based on which the growth rates for the three independent face, {111}, {100} and {110} were estimated using the equations below (Ma, et al., 2008, Wang et al, 2008):

$$G_1 = 7.753\times10^{-7}\,\sigma^{1.5};\ G_2 = 1.744\times10^{-6}\,\sigma^{1.5};\ G_3 = 1.124\times10^{-6}\,\sigma^{1.5} \quad (4)\sim(6)$$

The discretisation method, moment of classes, was used to solve the three-dimensional PB equation by extending the numerical solution procedure for a two-dimensional PB equation described. The three-dimensional size domain was discretised into n_1, n_2, n_3 classes, i.e., CL_i (i=1, n_1), CL_j (j=1, n_2), CL_k (k=1, n_3). The corresponding size and characteristic dimensional length of each class in each dimension are $\Delta x_i = x_i - x_{i-1}$, $\Delta y_j = y_j - y_{j-1}$, $\Delta z_k = z_k - z_{k-1}$ and $\bar{x}_i=(x_{i-1}+x_i)/2$, $\bar{y}_j=(y_{j-1}+y_j)/2$, $\bar{z}_k=(z_{k-1}+z_k)/2$, respectively. Therefore, a system of $n_1 \times n_2 \times n_3$ three-dimensional classes was formed with the class $Cl_{i,j,k}$, being delimited by (x_i, x_{i-1}), (y_j, y_{j-1}), (z_k, z_{k-1}). By integrating Eq. (3) over class $Cl_{i,j,k}$ of x, y and z, a set of $n_1 \times n_2 \times n_3$ ordinary differential equations can be formed as follows:

$$\frac{1}{V_T(t)}\frac{d}{dt}\left[N_{i,j,k}(t)V_T(t)\right]+[FX^O_{i,j,k}(t)-FX^I_{i,j,k}(t)]+[FY^O_{i,j,k}(t)-FY^I_{i,j,k}(t)] \\ +[FZ^O_{i,j,k}(t)-FZ^I_{i,j,k}(t)]=0 \quad (7)$$

where $N_{i,j,k}(t)$ is the number of crystals in the class $Cl_{i,j,k}$:

$$N_{i,j,k}(t)=\int_{x_{i-1}}^{x_i}\int_{y_{j-1}}^{y_j}\int_{z_{k-1}}^{z_k}\psi(x,y,z,t)\,dx\,dydz \quad (8)$$

and the first term on the left hand side of Eq. (12) is the accumulation term and can be rewritten as

$$\frac{1}{V_T(t)}\frac{d}{dt}\left[N_{i,j,k}(t)V_T(t)\right]=\frac{N_{i,j,k}(t)}{V_T(t)}\frac{dV_T(t)}{dt}+\frac{N_{i,j,k}(t+1)-N_{i,j,k}(t)}{\Delta t} \quad (9)$$

and the second, third and fourth terms on the left hand side of Eq. (12) are the net flows of crystals in class $Cl_{i,j,k}$ due to crystal growth with the superscripts, O and I, denoting the crystal flowing outletting from and inletting into the $Cl_{i,j,k}$ class:

$$FX^O_{i,j,k}(t)-FX^I_{i,j,k}(t)=\int_{x_{i-1}}^{x_i}\int_{y_{j-1}}^{y_j}\int_{z_{k-1}}^{z_k}\frac{\partial}{\partial x}\left[G_1(x,t)\psi(x,y,z,t)\right]dx\,dy\,dz \quad (10)$$

$$FY^O_{i,j,k}(t)-FY^I_{i,j,k}(t)=\int_{x_{i-1}}^{x_i}\int_{y_{j-1}}^{y_j}\int_{z_{k-1}}^{z_k}\frac{\partial}{\partial y}\left[G_2(y,t)\psi(x,y,z,t)\right]dx\,dy\,dz \quad (11)$$

$$FZ^O_{i,j,k}(t)-FZ^I_{i,j,k}(t)=\int_{x_{i-1}}^{x_i}\int_{y_{j-1}}^{y_j}\int_{z_{k-1}}^{z_k}\frac{\partial}{\partial z}\left[G_3(z,t)\psi(x,y,z,t)\right]dx\,dy\,dz \quad (12)$$

The crystal flow fluxes in x direction (Eq. (15)) can be calculated using the following formulation and similar formulation can be obtained for other two directions:

$$FX^I_{i,j,k}=G_1(\bar{x}_{i-1},t)\left[a_{i-1}N_{i-1,j,k}(t)+b_{i-1}N_{i,j,k}(t)\right] \quad (13)$$

$$FX^O_{i,j,k}=G_1(\bar{x}_i,t)\left[a_iN_{i,j,k}(t)+b_iN_{i+1,j,k}(t)\right] \quad (14)$$

where $a_i = \Delta x_{i+1}/[\Delta x_i(\Delta x_{i+1}+\Delta x_i)]$ and $b_i = \Delta x_i/[\Delta x_{i+1}(\Delta x_{i+1}+\Delta x_i)]$ with boundary conditions for crystal flow fluxes as:

$$FX^I_{1,j,k}(t)=FY^I_{i,1,k}(t)=FZ^I_{i,j,1}(t)=0 \quad (15)$$

$$FX^O_{1,j,k}(t)=FY^O_{i,1,k}(t)=FZ^O_{i,j,1}(t)=0 \quad (16)$$

The solid concentration, $C_S(t)$, in unit volume of suspension in a well-mixed batch crystalliser for a given time, t, can be calculated by

$$C_S(t)=\frac{\rho_s}{M_s}\int_x\int_y\int_z x\cdot y\cdot z\cdot\psi(x,y,z,t)\,dx\,dydz \quad (17)$$

whereas, with negligible effect of crystallisation and temperature variation on total volume, the volume of suspension, $V_T(t)$, can be calculated by $V(0)/[1-M_s/\rho_s\,C_s(t)]$, and the solute concentration, C(t), can be estimated with $C(0) - C_S(t)/[\,1-M_s/\rho_s\,C_s(t)]$.

The growth of individual faces over the time interval Δt, {111}, {100} and {110} are used to predict the new locations of the corresponding crystal faces. The updated normal distances of individual faces, together with their corresponding face orientation, can be used to form a set of linear equations and the solution of these equations will generate the coordinates of all corners on the crystal.

4. Results and Discussions

It was found that after 1000 seconds, the normal distance to the {111} face from the geometric centre of the crystal has been doubled. However the normal distance to the {100} face has changed from about 10μm to around 40μm, i.e. about four times.

.

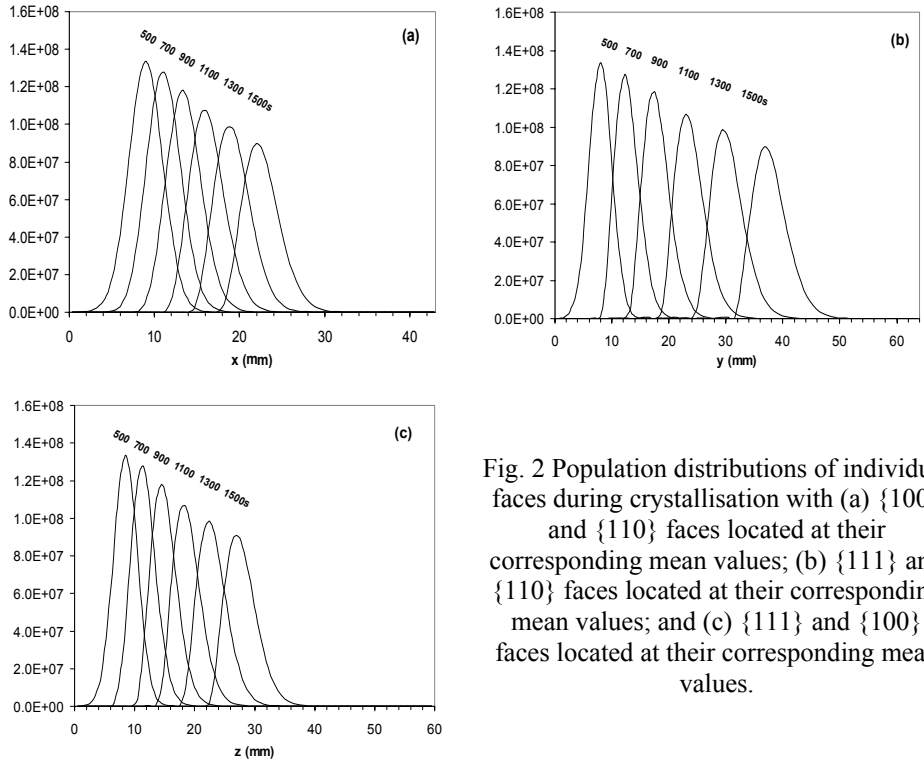

Fig. 2 Population distributions of individual faces during crystallisation with (a) {100} and {110} faces located at their corresponding mean values; (b) {111} and {110} faces located at their corresponding mean values; and (c) {111} and {100} faces located at their corresponding mean values.

By fixing two characteristic parameters of the morphological PB model at their corresponding mean values, the population distributions of the third parameter at different crystallisation times (500, 700, 900, 1100, 1300 and 1500 seconds) are plotted in Fig. 2. It was found that the assumed initial Gaussian distributions of population were preserved with the curve-fitting parameter, R^2, being over 0.99. During crystallisation process, the maximum value of population was decreased from 1.33×10^8 at 500 seconds to 8.96×10^7 at 1500 seconds. The corresponding FWHM (full width at half maximum) values were increased from 4μm at 500 seconds to 4.23μm at 1500 seconds for the {111} face, 5.83μm for the {100} face, and 5.03μm for the {110} face.

Fig.3 shows the evolution with time of the constructed crystal shape. It shows that faces {100} and {110} eventually disappear and the crystal will become pure octahedral, diamond-like shaped. Such pure octahedral shaped crystals for potash alum were observed in experiment by Amara et al (Amara, et al., 2004). The crystal shapes predicted at times of 1100s and 1300s (Fig. 3) are very close to the morphology of potash alum crystal obtained from single crystal study(Klapper, et al., 2002). It was found that the areas of faces {100} and {110} were reduced to very small values with increasing crystallisation time whilst the area of the dominated face {111} has increased dramatically. It was also found that the surface areas of potash alum crystal based on the simulated results were much larger than the ones with the equivalent diameter of sphere.

As surface area is one of the very important properties, the big difference of surface areas presented here indicated the necessity of using the morphological PB model to capture important crystal properties even for a sphere-like shape like this one.

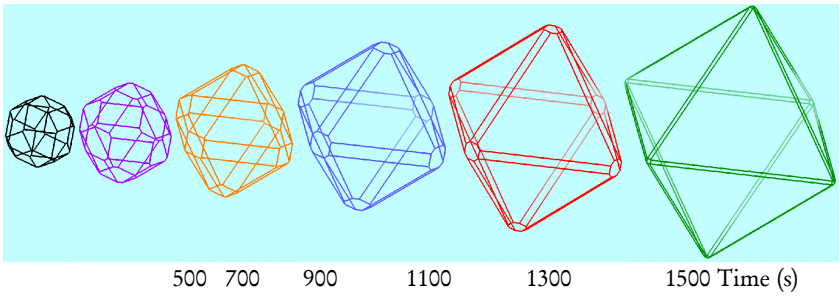

Fig. 3 Skeletons showing the modelled morphological evolution with time

5. Concluding Remarks

Crystals, particularly organic crystals of speciality chemicals such as pharmaceuticals, grown from solution can produce materials with specific crystal shapes and size distributions which substantially affect product performance and downstream processing. Traditionally, PB modelling has been conducted mainly for a mono-dimension without considering the crystal morphology. A few recent attempts in literature to consider crystal shape have been restricted to two dimensions only. In this study, a methodology to predict the variations of individual crystal faces during crystallisation has been developed by integrating crystal morphology into morphological PB modelling with multiple size dimensions. The methodology was introduced by reference to potash alum for which literature data is available for validation. The simulation results were qualitatively confirmed by literature data.

Acknowledgements

The study is funded by UK Engineering and Physical Sciences Research Council (EP/C009541) with support of Malvern Instruments, Pfizer, AstraZeneca and Nexia.

References

N. Amara, B. Ratsimba, A. Wilhelm, H. Delmas, 2004, Ultrasonics Sonochemistry, 11, 17-21.
H. Briesen, 2006, Chem Eng Sci, 61, 104-112.
F.B. Campos, P.L.C. Lage, 2003, Chem Eng Sci, 58, 2725-2744.
H. Klapper, R.A. Becker, D. Schmiemann, A. Faber, 2002, Crystal Res Tech, 37, 747-757.
R. Lacmann, A. Herden, C. Mayer, 1999, Chem Eng Tech, 22, 279-289.
C.Y. Ma, X.Z. Wang, K.J. Roberts, 2008, AIChE J, 54, 209-222.
C.Y. Ma, X.Z. Wang, K.J. Roberts, 2007, Adv Powder Techn, 18, 707-723.
D.L. Ma, D.K. Tafti, R.D. Braatz, 2002, Ind Eng Chem Res, 41, 6217-6223.
F. Puel, G. Fevotte, J.P. Klein, 2003a, Chem Eng Sci, 58, 3715-3727.
F. Puel, G. Fevotte, J.P. Klein, 2003b, Chem Eng Sci, 58, 3729-3740.
W.T. Read, W. Shockley, 1950, Phy Review, 78, 275-289.
R.I. Ristic, B. Shekunov, J.N. Sherwood, 1996, J Crystal Growth, 160, 330-336.
R.I. Ristic, B.Y. Shekunov, J.N. Sherwood, 1997, J Crystal Growth, 179, 205-212.
A. Vanderheijden, J.P. Vandereerden, 1992, J Crystal Growth, 118, 14-26.
X.Z. Wang, J. Calderon De Anda, K.J. Roberts, 2007, Chem Eng Res Des, 85, 921-927.
X.Z. Wang, C.Y.Ma, K.J. Roberts, 2008, Chem Eng Sci, 63, 1173-1184.
D. Zhang, G. Lu, 2004, Pattern Recognition, 37, 1-19.